Themed Issue: Drug Addiction - From Basic Research to Therapies
Guest Editors - Rao Rapaka and Wolfgang Sadée

Homology Modeling of Opioid Receptor-Ligand Complexes Using Experimental Constraints

Submitted: March 11, 2005; Accepted: April 29, 2005; Published: October 5, 2005

Irina D. Pogozheva,[1] Magdalena J. Przydzial,[1] and Henry I. Mosberg[1]

[1]Department of Medicinal Chemistry, College of Pharmacy, University of Michigan, Ann Arbor, MI 48109

ABSTRACT

Opioid receptors interact with a variety of ligands, including endogenous peptides, opiates, and thousands of synthetic compounds with different structural scaffolds. In the absence of experimental structures of opioid receptors, theoretical modeling remains an important tool for structure-function analysis. The combination of experimental studies and modeling approaches allows development of realistic models of ligand-receptor complexes helpful for elucidation of the molecular determinants of ligand affinity and selectivity and for understanding mechanisms of functional agonism or antagonism. In this review we provide a brief critical assessment of the status of such theoretical modeling and describe some common problems and their possible solutions. Currently, there are no reliable theoretical methods to generate the models in a completely automatic fashion. Models of higher accuracy can be produced if homology modeling, based on the rhodopsin X-ray template, is supplemented by experimental structural constraints appropriate for the active or inactive receptor conformations, together with receptor-specific and ligand-specific interactions. The experimental constraints can be derived from mutagenesis and cross-linking studies, correlative replacements of ligand and receptor groups, and incorporation of metal binding sites between residues of receptors or receptors and ligands. This review focuses on the analysis of similarity and differences of the refined homology models of μ, δ, and κ-opioid receptors in active and inactive states, emphasizing the molecular details of interaction of the receptors with some representative peptide and nonpeptide ligands, underlying the multiple modes of binding of small opiates, and the differences in binding modes of agonists and antagonists, and of peptides and alkaloids.

KEYWORDS: ligand docking, modeling, opioid receptors, opioid ligands, pharmacophore model

Corresponding Author: Henry I. Mosberg, Department of Medicinal Chemistry, College of Pharmacy, University of Michigan, 428 Church St, Ann Arbor, MI 48109-1065. Tel: (734) 764-8117; Fax: (734) 763-5595.

INTRODUCTION

Clinical interest in opioid receptors (ORs) is related to the development of strong analgesics without potential for abuse or adverse side effects. This task, however, cannot be accomplished without understanding the differences in the OR subtypes as well as the modes of interactions of drugs/ligands with these receptors.

Research on ORs was significantly advanced by the cloning of δ-opioid (DOR), μ-opioid (MOR), and κ-opioid (KOR) receptors in the early 1990s.[1,2] Sequence comparison confirmed that ORs belong to the rhodopsin-like family of G-protein-coupled receptors (GPCRs).[1] ORs are composed of a core domain of 7 transmembrane (TM) α-helices and an adjacent, peripheral helix 8 (IL4), are connected by 3 extracellular (EL1, EL2, EL3) and 3 intracellular (IL1, IL2, IL3) loops, and contain glycosylated N-terminal and palmitoylated C-terminal domains of different sizes. ORs demonstrate high sequence identity in their TM domain (73%-76%) and in ILs (63%-66%) and large divergence in N- and C-terminal domains and ELs (34%-40% identity).

ORs are activated by either endogenous peptides or exogenous opiates. The endogenous opioid peptides such as β-endorphin, Leu- and Met-enkephalins, dynorphins, and many others are mainly derived from 3 precursors, pro-opiomelanocortin, proenkephalin, and prodynorphin. They are found mostly in central and peripheral neurons, and also in gut, lungs, spleen, heart, and blood cells.[3,4] In addition, several opioid peptides have been isolated from cow's milk and frog skin. The majority of opioid peptides contain the core tetrapeptide, Tyr-Gly-Gly-Phe, important for high affinity and bioactivity.[5] In frog-skin-derived peptides the "Gly-Gly" motif is substituted by D-stereoisomers of Ala, Met, or Ile. Pharmacological studies indicate that no family of endogenous peptides is exclusively associated with a particular receptor type.[6]

The need for highly selective and potent agonists and antagonists stimulated the design of numerous synthetic opioid peptides. Thousands of linear peptides have been synthesized, some of them demonstrating subtype selectivity. To improve ligand selectivity, conformational and topographical constraints have been incorporated into the peptide ligands, and several highly selective cyclic peptides have been generated.[5] The first highly δ-selective enkephalin

analog, the cyclic peptapeptide Tyr-c[DPen-Gly-Phe-D-Pen]OH (DPDPE), was designed using cyclic bridging via a disulfide and the topographically constrained D-amino acid D-Pen (Pen, penicillamine, β'β-dimethylcysteine).[7] μ-Selective cyclic dodecapeptide antagonists lacking the characteristic "Tyr-Gly-Gly-Phe" motif were developed based on the somatostatin sequence.[8,9] Active cyclic analogs of dynorphin A(1–11) and (1–13) were also produced by incorporating disulfide cross-link between cysteines in positions 5–11, 5–10, 5–9, 4–9, 6–10, 8–12, 8–13, 5–13,[10] between L, D-Cys and L, D-Pen in positions 5–11,[11] or by introduction of a lactam bridge between residues in positions 2–5,[12] 2–6, 3–7, or 5–8.[13] Most of these cyclic dynorphin analogs demonstrated high κ- and μ-affinity, and some, such as c-[D-Asp3, Lys7]DynA(1–11)NH_2 were moderately κ-selective.[13] The properties of these cyclic opioid peptides have been reviewed in detail by Hruby and Agnes.[5]

Synthetic nonpeptide opioid ligands belong to several structural classes, such as morphine analogs, bimorphinans, benzomorphans, phenylpiperidines, phenylpiperazines, 4-anilinopiperidine, methadone analogs, and arylacetamides.[14] The correspondence of key structural elements between opioid peptides and nonpeptides is not always obvious.

Except for the recently crystallized rhodopsin,[15,16] structural data on individual GPCRs, including ORs, are limited; therefore theoretical modeling remains an important tool for structure-function analysis of these receptors.[17] Modeling of ligand-receptor complexes is usually performed to achieve several goals: to explain the experimental results of ligand-receptor interactions; to understand the molecular mechanism of ligand selectivity and ligand agonist or antagonist properties; or to propose a receptor-based pharmacophore model for agonists and antagonists that can provide a basis for virtual screening of future drug leads and for structure-based drug design.

Depending on the research goal, the modeling algorithm can include any of the following steps, which will be described in further detail: (1) identification of the bioactive conformation of the opioid ligands based on their structure activity relation (SAR) and theoretical and experimental conformational studies; (2) experimental studies of receptor-ligand interactions to uncover key ligand-receptor contacts; (3) homology modeling of the receptor using the rhodopsin template and additional experimental constraints appropriate for a specific receptor in its active or inactive states; (4) ligand docking using experimentally determined key interactions across a set of structurally similar and dissimilar ligands to develop, independently, pharmacophore models for agonist and antagonists.

Bioactive Conformation of Opioid Ligands

Small alkaloids, such as morphine analogs (eg, morphine, naltrindole (NTI), oxymorphinole (OMI), spiroindanyloxymorphone (SIOM), naloxone, naltrexone, etorphine) and benzomorphans (bremazocine), as well as the larger bimorphinans (norBNI) and phenylpiperazines (BW373U86) (Figure 1), have relatively rigid structures that must represent their bioactive conformations.[18-21] Some rotational flexibility is allowed around a few rotatable bonds such as in the N-allyl or N-cyclopropylmethyl groups of morphinans, in C-7 substituents of oripavines, at fumatate moiety of β-FNA, and the diethylamide group of BW373U86. The possible uncertainties resulting from such limited flexibility can be analyzed during ligand docking.

Selective agonists based on the arylacetamide scaffold are more conformationally flexible. Rotation around 3 single bonds (ie, χ1, χ2, and χ3 angles, see Figure 1) dramatically changes the relative orientation of the key pharmacophore elements of U69,593: the ammonium moiety of its pyrrolidine ring, the amide carbonyl group, and the phenyl group. The bioactive conformation of arylacetamides can be deduced from the superpositions of different analogs with structural restrictions introduced at the corresponding dihedral angles.[22] The reported X-ray structure of U69,593[23] overlaps well with all low-energy conformations of structurally restricted arylacetamides and therefore can be proposed as the bioactive conformation.

In the crystal structure of the μ-selective agonist cis(+)-3-methylfentanyl,[18] the central piperidine ring is in a chair conformation with 4-phenylpropanamide and N-phenethyl (in its extended conformation) in equatorial positions. Molecular dynamics simulations indicate high populations of different orientations of fentanyl analogs owing to torsional flexibility at 3 angles that define orientation of N-phenethyl (χ1 and χ2) and of N-phenylpropanamide (χ3).[24] Docking of fentanyl analogs into a MOR model can be used to unequivocally identify the receptor-bound conformation of the ligand.

Linear opioid peptides are very flexible and can adopt a variety of different conformations in solution. To determine the bioactive conformations of opioid peptides, a great number of cyclic peptides have been synthesized.[5] Small cyclic peptides are particularly useful, as they adopt a restricted number of conformations that can be theoretically predicted or experimentally determined. Moreover, introduction of conformational constraints into small cyclic ligands allows exploration of the structural requirements for opioid peptides to effectively and selectively interact with ORs. During the past few years we have developed a large number of cyclic tetrapeptides with high affinity toward MOR, DOR, and KOR.[25-33] In particular, the cyclic tetrapeptides JOM13 (Tyr-c[D-Cys-Phe-D-Pen]OH, cyclized through a disulfide bond) and JOM6 (Tyr-c[D-Cys-Phe-D-Pen]NH2, cyclized via an ethylene dithioether), are highly potent and selective for DOR and MOR, respectively.[25] The design of κ-selective tetrapeptides based upon the same type scaffold as JOM13 and JOM6 has

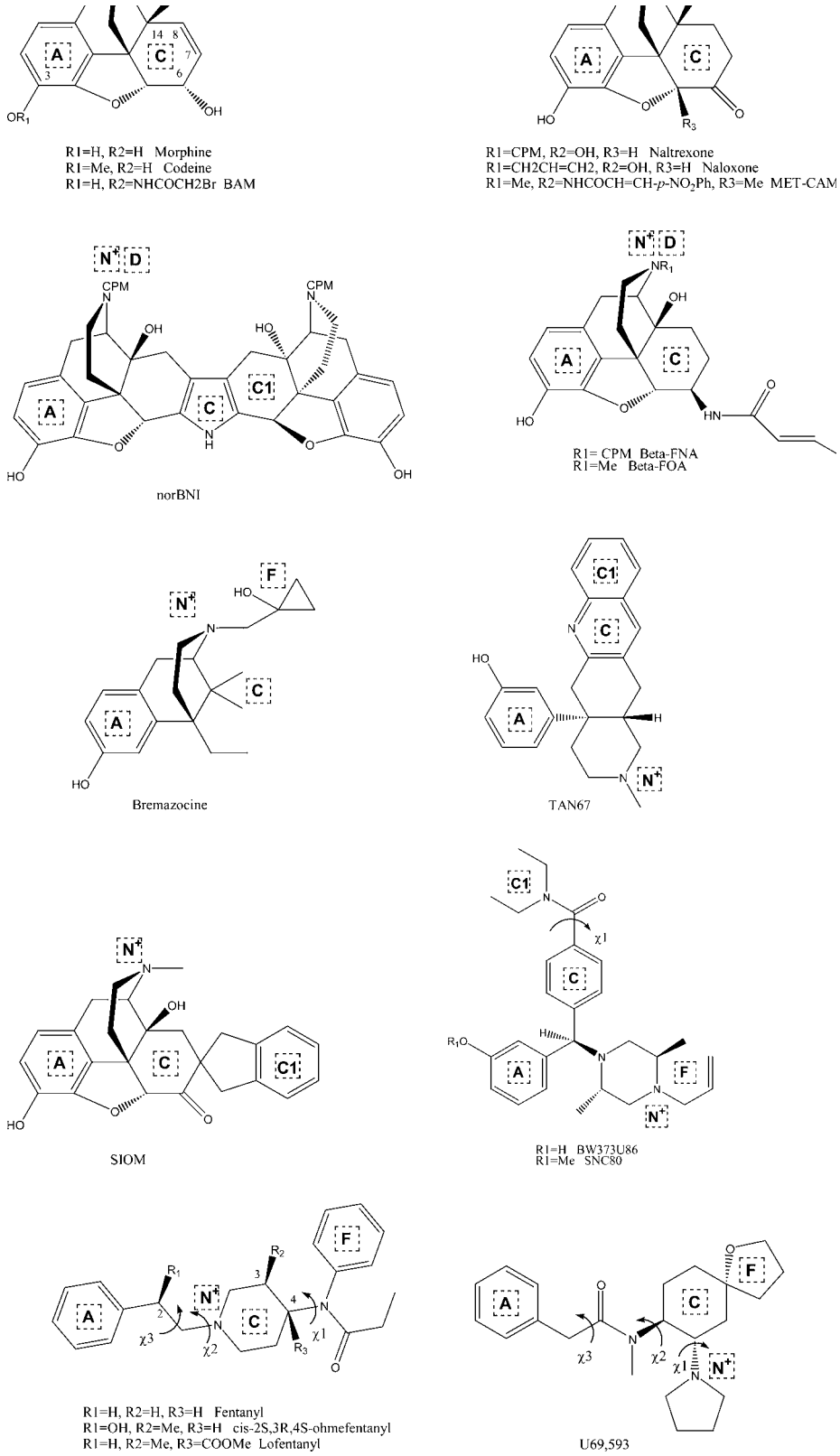

Figure 1. Structures of opioid ligands. Pharmacophore elements, "N+," "A," "C," "C1," and "F" are indicated in the boxes.

been more challenging. Although cyclic tetrapeptides with high κ-selectivity have not been obtained, the cyclic tetrapeptide, MP16 (Tyr-c[D-Cys-Phe-D-Cys]NH2, cyclized via a disulfide) demonstrates nanomolar affinity to KOR.[26]

Subsequent modifications of the parent tetrapeptides were directed toward elucidation of structural requirements for Tyr1 and Phe3 residues, which are key residues for recognition of cyclic tetrapeptides by ORs.[25-33] The following

conclusions were derived from these studies (Table 1). First, the importance of aromatic residues in positions 1 and 3 was confirmed for all selective peptides. Second, cyclization via an ethylene dithioether bridge favors MOR binding, while the smaller disulfide-containing cycle is preferred for peptide recognition by DOR and KOR. Third, restriction of the Phe3 side chain in the *trans* (χ1~180°) rotamer is favorable for MOR and KOR high binding affinity, while restriction of the Phe3 side chain in the *gauche*+ (χ1~-60°) conformation provides improved DOR affinity. Fourth, the presence of a C-terminal amide is important for ligand binding to MOR and KOR, while a free C-terminal carboxylate enhances DOR affinity. Fifth, the presence of D-Cys4 in place of D-Pen4 in the tripeptide cycle dramatically increases binding affinity to KOR, while retaining high affinity to MOR and DOR. A combination of SAR, X-ray, and nuclear magnetic resonance (NMR) studies, and computational analysis of the cyclic tetrapeptides allowed us to deduce the bioactive conformations of JOM13,[25,31] JOM6,[32,34] and MP16,[26] which appeared to be complimentary to the binding pockets of modeled ORs.[26,34,35]

Experimental Studies of Receptor-Ligand Interactions

Experimental studies useful for developing a crude topographical ligand-receptor interaction model include comparative affinity determination of ligands in receptor mutants, correlated replacements of ligand and receptor functional groups, covalent cross-linking of ligand to receptors, and the design of metal binding sites between ligand and receptors. Particularly important is the identification of specific interactions conferring ligand selectivity and agonist or antagonist properties.

Studies of OR chimeras and site-directed mutants revealed that the ligand binding pocket is located between TMs 2–7 and is covered by EL1, EL2, and EL3. Published mutagenesis data on ORs delineated a set of more than 20 residues in the TM α-bundle important for binding of opioid ligands.[36-38] It is assumed that conserved residues from TM 3–7 of ORs represent the common opioid pocket for the tyramine "message" part of opioid peptides and alkaloids, which triggers receptor transition to the active or inactive conformation, while subtype-specific residues from TMs 5–7, EL1, EL2, and EL3 contact the "address" part of the ligands, providing recognition of selective ligands by the corresponding receptors.[39,40]

The residues from the binding pocket, essential for ligand binding, are mostly conserved across the ORs and include Asp(3.32), Tyr(3.33), Lys(5.39), Phe(5.47), Trp(6.48), Ile(6.51), His(6.52), Ile(6.53), Ile(7.39), and Tyr(7.43).[41-50] Binding determinants for small alkaloids (morphine, codeine) reside in TMs 5–7.[51] Variable binding pocket residues confer selectivity. For example, Lys108 in EL1 of DOR prevents binding of the μ-selective DAMGO[52]; residues from EL2 and EL3 confer the selectivity of dynorphin to KOR[39,53-55]; and variable residues from EL3 and adjacent helices, particularly Lys303(6.58), Trp318(7.35), and His319(7.73) of MOR and the corresponding Trp284(6.58) and Leu300(7.35) and His301(7.36) of DOR are important for selective binding of morphine, DAMGO, and fentanyl analogs to MOR,[56-58] and of DPDPE, SNC80, and TAN67 to DOR.[37,59,60] Glu297(6.58) in KOR is involved in binding of norBNI.[61]

Several conserved residues in the binding pocket, such as Asp(3.32), Tyr(3.33), Lys(5.39), His(6.52), Trp(6.48), and Tyr(7.43), as well as divergent residues in positions 6.58 and 7.35, also participate in receptor activation.[42,44,47,56,62-65] Of interest, in the mutants D128K(3.32) of DOR and H297Q(6.52) of MOR, the antagonist naloxone demonstrates agonistic properties.[47,62] In addition, the H287Q(6.52) mutant of MOR is more resistant to β-FNA irreversible binding,[66] which acts at this mutant as a partial agonist.[66]

In many cases it is difficult to unequivocally distinguish between residues from the binding site, an allosteric regulation site, or those involved in receptor structural changes without detailed analysis of ligand-receptor interactions. To date, direct contacts between opioid ligands and corresponding receptor residues have been documented in only a few cases. Among these are interactions between the basic N^+ of the opioid ligand and Asp147(3.32) in MOR,[50] between the fumarate moiety of the irreversible μ-antagonist β-FNA and Lys233(5.39) in MOR,[67] and between the N-17' basic nitrogen of norBNI and the acidic Glu297(6.58) of KOR[61] or the

Table 1. Structural Requirements for Cyclic Tetrapeptides With High Affinity to μ-, δ-, and κ-receptors

Receptor (ligand)	K_i ± SEM (nM)	Residue 3	Residue 4	C-Terminus	Bridge	Side Chain Rotamer*		
						Residue 3	Residue 2	Residue 4
μ (JOM6)	0.17 ± 0.02	Phe^3	$D\text{-}Pen^4$	$CONH_2$	S-Et-S	trans	trans	trans
δ (JOM13)	1.3 ± 0.06	Phe^3	$D\text{-}Pen^4$	COO^-	S-S	gauche+	trans	gauche+
κ (MP16)	38.7 ± 1.84	Phe^3	$D\text{-}Cys^4$	$CONH_2$	S-S	trans	gauche+	gauche-

**trans* side chain rotamer corresponds to χ1~180°; *gauche*+ to χ1~-60°; *gauche*- to χ1~+60°.

corresponding K303E(6.58) of the MOR mutant.[68,69] Recently, MOR mutagenesis combined with comparison of affinity of different fentanyl analogs revealed interactions of the 2'-OH of cis(2'R,3R,4S)-ohmefentanyl and Tyr138(3.33), and the proximity of Trp318(7.35) and His319(7.36) to the *p*F-phenyl group of p-fluorofentanyl.[57,58]

Recent mutagenesis studies have allowed us to develop a topographical scheme of key ligand-receptor contacts between JOM6 and MOR,[34] which is presented in Figure 2. These studies provided evidence for the formation of a metal binding site by Asp216(EL2) and His319(7.36) near the peptide binding pocket of MOR and uncovered new interactions between MOR and its selective cyclic tetrapeptide, JOM6. In particular, Zn^{2+} binding sites were engineered between MOR mutants and His-substituted analogs of JOM6: [His1]JOM6-V300C-H297 and [His3]JOM6-G213C-T315C. Also, reciprocal substitution of receptor and ligand functional groups indicated the proximity between the C-terminal amide of JOM6 and Glu229 (5.35) and between Phe3 of JOM6 and Trp318 (7.35). Such unambiguous structural constraints between receptor and ligand atoms are essential for accurate modeling of the receptor ligand complexes. These constraints were recently employed for distance geometry calculations of complexes of MOR with the bimorphinan antagonist norBNI,[70] and with the cyclic tetrapeptide agonist JOM6.[34]

Homology Modeling of Opioid Receptors

During the mid to late 1990s several models of opioid receptors were proposed based on the nonhomologous bacteriorhodopsin or low resolution electron microscopy maps of rhodopsin.[22,24,57,71-77] We developed at that time a computational approach for modeling the transmembrane, 7 α-helical bundle of GPCRs that employed an iterative distance geometry refinement with an evolving system of interhelical hydrogen bonding constraints[78] and applied it to the

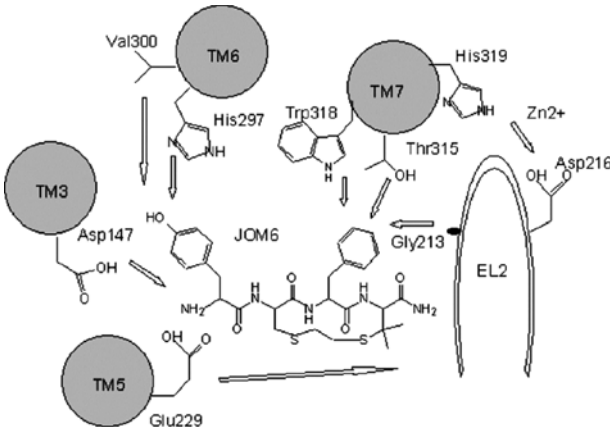

Figure 2. Schematic drawing of the interactions of JOM6 with MOR.

modeling of MOR, DOR, and KOR[40] and other GPCRs.[79] The rhodopsin model calculated with this approach was close to the subsequently published crystal structure (root mean square deviation [rmsd] 2.88 Å for 186 Cα-atoms in the TM domain). Other methods for GPCR modeling that do not rely on a structural template include MembStruck[80] and PREDICT,[81] which also produced realistic models of rhodopsin (rmsd of 3.1 Å and 3.87 Å, respectively, vs the rhodopsin X-ray structure in the 7TM domain) and were used to model other GPCRs. Although such ab initio methods were able to achieve medium accuracy in the modeling of the α-helical TM domains of GPCRs, they failed to correctly predict the structure of the receptor loops.[80] This could seriously affect the analysis of ligand-receptor interactions, especially for peptide ligands since ELs are known to participate in contacts conferring ligand selectivity.[82,83] Nevertheless, these various methods yielded results that were consistent with available ligand SAR and confirmed the ligand-based pharmacophore models.[14,35]

It has been widely demonstrated that the most reliable computer-based technique for generating 3-dimensional models is via homology modeling.[84] The publication of the rhodopsin crystal structure[16,85] has made homology modeling of receptors from the rhodopsin-like family possible,[86-89] and several opioid receptor models based on the rhodopsin template have subsequently been produced.[37,65,88,90,91] Knowing the structural template, the homology models can be generated using MODELER,[92,93] or publicly available Web servers, such as SWISS-MODEL, EsyPred3D, Robetta, CPHmodels, or SDSC1,[94-98] or downloaded from databases, such as ModBase.[99]

The accuracy of comparative modeling is highly dependent on the sequence identity between the target sequence of interest and the template sequence. High accuracy comparative modeling (rmsd ~1Å) can be achieved when the target and template proteins have sequence identity of more than 50%, while the accuracy drops when the identity of target and template sequences is less than 30%.[84] The opioid receptor sequences have only ~20% identity to rhodopsin for all residues and ~29% identity in TM segments. Therefore, automated homology modeling of ORs is likely to result in numerous errors. The major source of errors is from sequence misalignment,[81,100,101] which can be expected in areas of low sequence identity and in regions of helical distortions. Helical irregularities are indeed observed in the crystal structure of rhodopsin, which exhibits a fragment of 3_{10} helix in TM7 and α-aneurisms (one residue insertion) in TM2 and TM5, as well as proline-induced kinks in TMs 1, 2, 4, 5, 6, and 7.[102] These distortions in α-helices may not be present in other GPCRs. Other sources of errors are the divergent loops, which in many cases should be constructed ab initio.[103] Further, the α-helices of modeled proteins may have altered lengths, positions, and orientations relative to

the template structure. Indeed, a sequence homology of ~20% between proteins suggests ~1.6 to 2.3 Å rmsd within the helical core, caused by helical shifts.[104]

Another problem is related to conformational rearrangement of the receptor during activation. The crystal structure of rhodopsin represents the inactive conformation in complex with the covalently bound inverse agonist, 11-cis-retinal. This structure can be used for homology modeling of the antagonist-bound inactive receptor state; however, the active states of rhodopsin and other GPCRs have been shown to differ from the inactive conformations.[15,105] The accumulated data from mutagenesis, cross-linking, electron paramagnetic resonance spectroscopy (EPR), and fluorescence studies suggest that different rhodopsin-like GPCRs share a common active conformation[106] in which TM6 undergoes a significant rigid-body motion in a counterclockwise direction, as viewed from the extracellular side.[107-109] This results in a significant shift of the intracellular end of TM6 outward from TM3[109,110] and TM7,[111,112] and toward TM5,[113] opening a cleft on the cytoplasmic surface of the α-bundle for binding of G-proteins.[105,114] A relatively smaller motion of TM3 and some conformational changes in the extracellular ends of TMs 1, 2, and 7 have also been observed.[109,115-120] Random mutagenesis of DOR provided evidence that the conformational transition originates at the ligand binding pocket near the extracellular ends of TM5, TM6, and EL3 and propagates through TMs 3, 6, and 7 down to a cytoplasmic switch between TMs 6 and 7.[65] Moreover, experimental studies of different GPCRs (eg, rhodopsin, β-adrenoreceptors, DOR) indicate that a conformational transition of the receptor may involve multiple intermediate states.[107,109,113,121-126] Therefore, agonists of different structural types may generate different activated states of receptors, which could be recognized by specific proteins involved in distinct transduction and regulation pathways.

Unfortunately, the existing methods for energy optimization, including molecular dynamics or distance geometry refinement, are unable to correct alignment errors or to reproduce helical shifts and distortions[127] and have been unsuccessful in modeling long irregular loops (>12 residues).[103] Some recent attempts demonstrated moderate improvement of homology models by combining several templates,[128] and some success in modeling helical shifts has resulted from using a new multiscale energy optimization algorithm.[129] Currently, model refinement requires human intervention and incorporation of additional information. For example, questionable target-template alignments in the area of helical distortions and in the loops of MOR have been clarified by mutagenesis data and construction of helix-loop metal binding sites.[34] In another example, initial homology models of tachykinin NK1 receptors were optimized in the area of the binding site by incorporation of distance constraints from the ligands in their bioactive conformation, using a new algorithm, MOBILE.[89,130] Accuracy of models of different functional states can also be improved by iterative distance geometry refinement with experimental interhelical restraints appropriate for only the active or inactive conformation derived from mutagenesis, cross-linking studies and design of metal binding sites together with ligand-receptor distance restraints.[70,88] For example, the important interhelical distance constraints for the positioning of TM6 in the activated receptor state can be deduced from recent data on the formation of disulfides between TM5 and TM6 in the m_3 muscarinic receptor upon agonist binding[131] and from the existence of an intrinsic allosteric Zn^{2+} binding site at the interface of TM5 and TM6 of the β_2-adrenergic receptor that facilitates agonist binding.[132] Additional constraints for adjusting helix packing in the activated state can be taken from the engineering of an activating metal-coordination center between TM3 and TM7 in β_2-adrenergic[133] and tachykinin receptors,[134] and also between TM2 and TM3 of the MC4 melanocortin receptor.[135]

Ligand Docking

Ligand docking should satisfy the surface complementarities between ligand and receptor and the key interactions deduced from mutagenesis studies of ligand-receptor interactions. In earlier modeling of receptor-ligand complexes, ligand docking was primarily done manually. In a recent review, Eguchi compared previously published models of receptor-ligand complexes for selective opioid agonists and antagonists that satisfied some experimental observations about receptor-ligand interactions and SAR of the ligands.[14] The comparison revealed that although the modeling was based on a common set of experimental data, the proposed models often contradicted each other in the manner of docking similar ligands, such as morphine and its analogs or κ-selective arylacetamides. It was unclear, however, whether such contradictions reflected the existence of multiple modes of ligand binding or appeared as a result of low accuracy of receptor modeling or inaccurate docking methods. Other important questions, such as differences between binding modes of peptides and alkaloids, and of agonists and antagonists were beyond the scope of the review by Eguchi. To answer these questions pharmacophore models should be developed separately for agonists and antagonists and docked to 3-D structures of the active and the inactive receptor conformations, respectively. Moreover, the models and docking algorithm should be relatively accurate.

Manual docking was recently used for homology- and knowledge-based models of inactive and activated GPCRs to find the position of ligands in the binding pockets that would agree with known ligand-receptor interactions.[88] The resulting models of antagonist-bound dopamine D_1,

muscarinic m_1, and vasopressin V_{1a} and agonist-bound DOR, dopamine D_3, and β_2-adrenergic receptors appeared to be suitable for the virtual screening of drug leads from databases of drug-like compounds with hit rates from 2% to 37%, depending on docking algorithm and scoring function used.[88]

Numerous programs, based on different methods, have been developed to automatically dock small ligands into proteins. These programs include DOCK,[136] GOLD,[137] FlexX,[138] FDS,[139] Glide,[140] LigandFit,[141] ICM,[142] and others. To improve results, the best docking algorithms are combined with different scoring functions.[143] Program performance is largely dependent on the accuracy of the receptor structure (especially in the case of modeled structures), on the flexibility of the ligand (number of rotatable bonds), and on the nature of the binding site.[143-145]

Receptor flexibility presents the major complication for automated docking. Almost all currently used programs perform semiflexible ligand docking, where the ligand is considered as flexible and the protein, as rigid. Such an approach is known to cause errors in computational studies. A few algorithms perform flexible docking in which limited protein flexibility, such as side chain motions in the active site, is incorporated. Some recent algorithms use an ensemble of protein structures, pregenerated by molecular dynamic simulations, to account for backbone or side chain flexibility in structure-based drug design,[146] but they are very computationally intensive. In a recent approach incorporated in MOBILE,[130] an ensemble of homology models was generated much faster using MODELER,[92] and the ligands were docked into an averaged binding site representation using AutoDock. To improve the results obtained, the docking solution that better reproduced the experimentally determined key ligand-receptor interactions was selected and was further utilized for the iterative refinement of the ligand-bound homology models. The refined antagonist-bound homology model of tachykinin neurokinin 1 (NK1) receptor obtained in this manner was successfully employed for the virtual search of NK1 antagonists from a database of lead-like compounds.[89,147]

We have applied a similar method, employing structural constraints to produce a more reliable homology model of the agonist-bound receptor state of MOR in complex with the μ-selective cyclic peptide agonist, JOM6.[70] This approach complied with the SAR and key ligand-receptor interactions of relatively flexible peptide ligands, which is a more complicated task than the docking of more conformationally rigid alkaloids. To reproduce the agonist-bound state, the receptor was calculated together with the bioactive conformation of the cyclic tetrapeptide using experimental distance constraints between ligand and receptor functional groups (see Figure 3). The active receptor conformation was calculated simultaneously using the interhelical distance constraints from the rhodopsin crystal structure to define the positions of TMs 1 to 5 and 7, receptor-specific H-bonds, and a set of experimental distance constraints between TMs 3 to 6 and TMs 5 to 6 to define the position of the largely flexible TM6. The latter constraints were derived from EPR, cross-linking studies, and from engineered metal binding sites.[108,131,132] The agonist bound conformations of DOR with JOM13 and of KOR with MP16 have also been calculated based on the MOR-JOM6 complex.[25,26] The receptor-bound conformations of JOM13 appeared to be very similar to one of the crystal forms of JOM13,[31] while the receptor-bound conformation of MP16 requires a

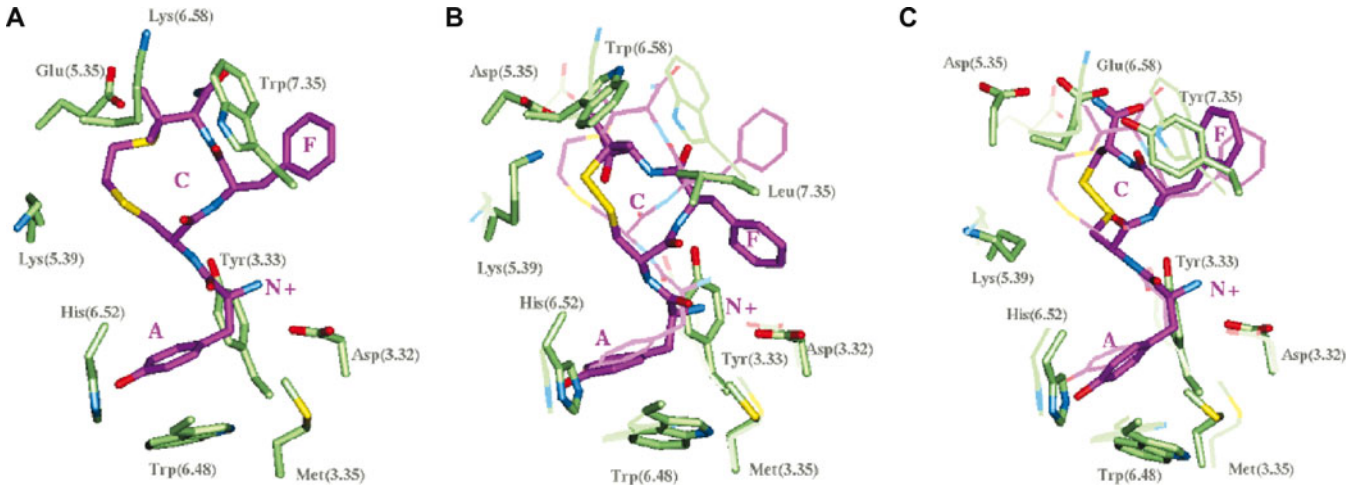

Figure 3. JOM6 in the binding pocket of agonist-bound conformation of MOR (A) and its superposition with JOM13 in DOR binding pocket (B) or with MP16 in the KOR binding pocket (C). Ligands (purple) and several key residues (colored by element), Asp(3.32), Tyr(3.33), Met(3.35), Glu/Asp/Asp(5.35), Lys(5.39), Trp(6.48), His(6.52), Lys/Trp/Glu(6.58), and Trp/Leu/Tyr(7.35) from MOR/DOR/KOR, respectively, are shown. JOM6 and MOR residues on B and C are presented by thin lines. Pharmacophore elements are indicated by N+, A, C, and F.

tripeptide cycle conformation that is ~2 kcal/mol higher in energy than the lowest energy state.[26]

The differences in binding cavity geometry among MOR, DOR, and KOR are related to the divergence in size, polarity, and charge of residues from the top of TMs 5 to 6, EL2, and EL3. The greatest difference is observed for KOR, whose 3-residue longer EL2 occupies more space between TM3 and TM7 and between TM3 and TM5. The binding pocket in KOR is consequently smaller in the regions between EL2 and TM7 and between EL2 and TM5. KOR also has several negatively charged side chains from EL2 (Asp204, Glu209, Asp216) and EL3 (Glu297) lining the binding cavity, which may have favorable ionic interactions with positively charged groups of κ-selective ligands.

In all 3 receptors, the positions of Tyr1 and of the central backbone cycle of tetrapeptide ligands are quite similar, but the orientations and interactions of the ligand Phe3 side chain are different (Figure 3). The common Tyr1 of the tetrapeptides interacts with conserved charged, aromatic, and aliphatic side chains from the binding pockets; the positively charged amine group forms H-bond and ionic interactions with Asp(3.32) and participates in amine-aromatic interactions with Tyr(3.33); and the Tyr1 phenolic hydroxyl can either be an H-acceptor from His(6.52) or an H-donor to -C=O of Ala(5.46), which is excluded from the usual system of intrahelical H-bonds because of the presence of an α-aneurism in TM5. The Phe3 of JOM13 adopts a *gauche*+ orientation that can be easily accommodated in the relatively hydrophobic environment of DOR between TM3, EL2, and TM7. In contrast, in MOR and KOR the corresponding area is partially filled by polar side chains from EL2. Therefore, the properties of the binding site in MOR and KOR favor the *trans* rotamer of Phe3, which is shifted closer to the extracellular surface. This is in agreement with the independently deduced pharmacophore model of cyclic tetrapeptides described above. In MOR, Trp318(7.35) forms an aromatic interaction with Phe3 of JOM6, supporting the important role of Trp318(7.35) in peptide binding to MOR.[56] Similarly, in KOR Tyr312(7.35) forms an aromatic interaction with Phe3 of MP16. The smaller size of the binding pocket in KOR relative to that in MOR, owing to extra residues inserted into EL2, prevents the binding of tetrapeptides with bulkier side chain substitutions in the Phe3 position. Indeed, the Trp3 analog of MP16, which cannot be accommodated between Phe214(EL2), Leu309(E3), and Tyr312(7.35) without some side chain and backbone shift, demonstrates decreased affinity.[26] On the other hand, the open space in MOR between the corresponding Phe221(EL2), Thr315(EL3), and Trp318(7.35) is large enough to accommodate the 1-Nal3-containing analog of JOM6, which shows high binding affinity.[148] The μ-, δ-, and κ-selectivity of opioid cyclic tetrapeptides is also largely affected by their C-terminal groups. The C-terminal -COO^- of JOM13 forms favorable ionic interaction with $N\varepsilon^+$ of Lys214(5.39) inside the DOR binding pocket, thus explaining the preference of a C-terminal free carboxylate for δ-selectivity. In the receptor-bound conformations of JOM6 and MP16, their carboxamide groups are spatially shifted closer to Glu210(5.35) of MOR or to Glu297(6.58) of KOR. Therefore, in order to avoid electrostatic repulsion between negatively charged groups, a neutral C-terminus is required for high affinity of μ- and κ- peptides.

The calculated agonist-bound and inactive state models of MOR, DOR, and KOR[26,34,70] were used for subsequent docking of nonpeptide agonists and antagonists, respectively. The ligands were positioned to provide the best overlap of the message tyramine (or tyramine-like) moieties and to satisfy known SAR and key receptor-ligand interactions, starting with the largest rigid ligands. Ligands from each structural class were analyzed separately. To account for the intrinsic flexibility of the receptor an ensemble of 5 to 10 models, calculated with a distinct set of spatial constraints, was used for ligand docking.

All opioid ligands interact with the same binding pocket; however, smaller ligands only partially occupy the available space, leaving some empty areas, which could be filled by several flexible "rotating" side chains from TMs and loops. The key rotating residues in the binding pocket include Asp(3.32), Met(3.36), Trp(6.48), Lys/Trp/Glu(6.58), and Trp/Leu/Tyr(7.35), with most of these being implicated in receptor activation.[56,64,65]

Similar to the cyclic tetrapeptides, nonpeptide agonists form an H-bond and ionic interaction between their amine N^+ and the *trans* rotamer of Asp(3.32), and a "stacking" interaction between aromatic tyramine ring and the indole ring of Trp(6.48), which can be slightly adjusted (χ2~0 ± 20°) to better accommodate different ligands (Figure 4). Unlike peptide ligands, the tyramine hydroxyl of nonpeptide agonists only interacts as an H-donor with backbone -C=O of Ala(5.46) but cannot interact with His(6.52). The

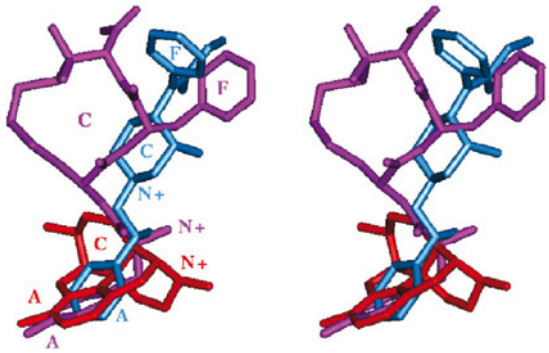

Figure 4. Stereoview of the superposition of JOM6 (purple), morphine (red), and cis-2S,3R,4S-ohmefentanyl (blue) in the binding pocket of the agonist-bound conformation of MOR. Pharmacophore elements are indicated by N+, A, C, and F.

functionally important α-hydroxyl or carbonyl at C-6 of opiates can form an H-bond with Lys(5.39) and Tyr(3.33), while a hydroxyl group at C-14 can form an H-bond with Tyr(3.33). The large aromatic moiety of δ-selective non-peptide agonists (SIOM, TAN67) interacts with the indole ring of Trp284(6.58) of DOR, which is consistent with the important role of Trp284(6.58) in binding of these ligands, as suggested from DOR mutagenesis.[37,59,60] Morphine and its small analogs can be positioned similarly to the larger opiates. However, in the large MOR binding pocket they can also occupy certain alternative positions. In particular, these different positions can allow the irreversible morphine analogs, MET-CAMO,[149] BAM, or S-activated dihydromorphine derivatives[150] to form a covalent bond with Cys321(7.38). The fentanyl analog, cis-2S,3R,4S-ohmefentanyl, can be positioned in the MOR binding pocket in an extended conformation,[18] with its phenethyl group imitating the tyramine part of opiates and peptides, and its 4-phenylpropanamide, forming aromatic interactions with Trp318(7.35), similar to Phe3 of peptides. Positioned this way, the fentanyl analog's N^+ can form an ionic interaction with Asp147(3.32) and an H-bond with Tyr148(3.33), while its 2'OH can form an H-bond with Tyr148(3.33). A similar arrangement of this fentanyl analog in MOR has been proposed[57] based on mutagenesis data.[57,58]

The comparison of the agonist-bound MOR[70] with our previously calculated inactive MOR[34] reveals that the major changes in the binding pocket are related to the side chain rotation of Trp293(6.48) from a rotamer with χ1~-60°, χ2~90° to a rotamer with χ1~-60° and χ2~0° (Figure 5). As a result, the indole ring of Trp293(6.48) relocates from the interface between TMs 6 to 7 to the interface between TMs 3 to 5–6, where it can form a "stacking" interaction with the aromatic ring of Tyr1 of JOM6. The agonist-induced Trp293(6.48) reorientation in MOR triggers a large TM6 rotation and shift, correlated reorientation of the Met151(3.35) side chain, ligand-dependent reorientations of the side chains of Asp147(3.32), Lys233(5.39), Lys303(6.35), and Trp318(7.35), and readjustment of some other helix positions. The important role of Trp(6.48) in the activation mechanism has been proposed previously based on mutagenesis data and on the experimentally documented movement of this side chain in photoactivated rhodopsin and in agonist-activated leukotriene receptors.[116,151-153] Of interest, the incorporation of different active state-specific experimental distance constraints between TMs 5 to 6[131,132] produced 5 different active conformations with deviation for the residues at the cytoplasmic ends of TM6 ranging from 7 to 11 Å, relative to the model of the inactive conformation.[34] Such flexibility of TM6 in the active conformation is consistent with the existence of ligand-dependent conformational substates, which have been observed upon binding of different agonists, antagonists, and inverse agonists to DOR[123-126] and other GPCRs.[107,113,121,122]

Inactive and agonist-bound bound states of receptor also differ in the relative position of 2 key residues, Asp(3.32) and His(6.52), the suggested partners for the tyramine moiety of opioid ligands. In the inactive state Asp(3.32) assumes a *gauche*+ rotamer (χ1~-60°), which, instead of forming an H-bond/ionic interaction with the protonated amine of the

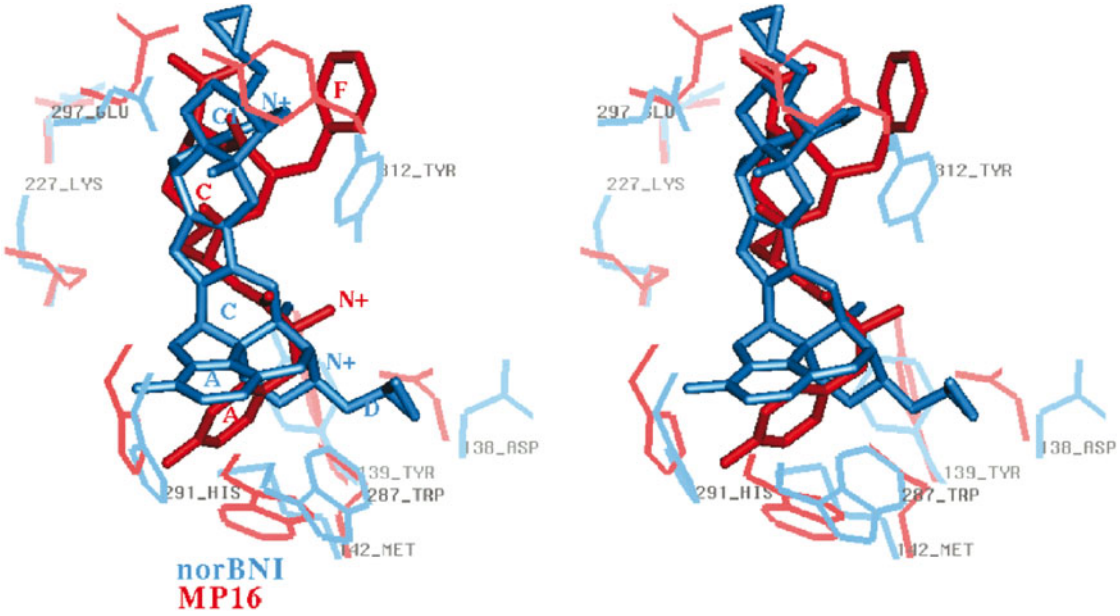

Figure 5. Stereoview of the superposition of MP16 in the binding pocket of the agonist-bound conformation of KOR (red) and norBNI in the binding pocket of the antagonist-bound conformation of KOR (blue). Only ligands and several important residues from MOR: Asp138(3.32), Tyr139(3.33), Met142(3.35), Lys227(5.39), Trp287(6.48), His291(6.52), Glu297(6.58), and Tyr312(7.35) are shown. Pharmacophore elements are indicated by N+, A, C, C1, and F.

ligand, participates in the formation of several H-bonds between residues of TMs 2, 3, 7: Thr(2.56), Gln(2.60), and Tyr(7.43). This H-bond network stabilizes the inactive receptor state. Indeed, D(3.32)N and D(3.32)K mutants that are incompatible with this H-bond network demonstrated increased constitutive activity.[44,62] In place of the agonist amine interaction with Asp(3.32), the positively charged amine of antagonists can instead form amine-aromatic interactions with the proximal Tyr(3.33), which is in agreement with the observed important role of this residue for ligand binding.[43] In the inactive state of ORs, His(6.52) is located between TM6 and TM3, forming H-bond and van der Waals interactions with the tyramine moiety of antagonists. In the agonist-bound state, His(6.52) is shifted toward TM5 owing to TM6 rotation, which breaks the H-bond with the tyramine hydroxyl of nonpeptide agonists. Moreover, in the inactive or ligand-free receptor states Trp/Leu/Tyr(7.35) can be oriented inside the receptor ($\chi 1 \sim 180°$), filling the binding cavity, while in the presence of large peptide agonists these residues are reoriented ($\chi 1 \sim -60°$), forming hydrophobic interactions with Phe3 of the peptides (see above).

The comparison of agonist and antagonist positioning in the agonist-bound and the antagonist-bound KOR conformations is demonstrated in Figure 5. Because of the differences in the interaction of the ligands with the key residues Asp138(3.32), Trp287(6.48), His291(6.52), and Tyr312(7.35), the antagonist norBNI is placed with its amine N^+ shifted more deeply into the pocket relative to MP16. The antagonist activity of morphine analogs is usually associated with an N-allyl or N-cyclopropylmethyl substituent on this amine N^+, while an N-methyl substituent is associated with agonists.[154] Because of added steric bulk and the deeper positioning in the pocket, the N-cyclopropylmethyl group of norBNI locks Asp138(3.32) and indole ring of Trp287(6.48) in the "inactive" orientations. Moreover, the central part of the "address" moiety of norBNI, which overlaps with the cyclic ring of tetrapeptides, forms favorable hydrophobic interactions with the *trans* (ie, inactive) rotamer of Tyr312(7.35), while its N-17' basic nitrogen forms an ionic interaction with Glu297(6.58), consistent with experimental observations.[61]

Such models of agonist and antagonist interactions with ORs can explain the observed larger effect of His(6.52) mutations and smaller effect of the D147A mutation on the binding of antagonists compared with agonists.[42,45] These models also provide a rationale for the recent observations that elimination of the N-terminal amino group converts several peptide agonists to antagonists.[155]

The analysis of modes of docking of peptide and nonpeptide agonists and antagonists into ORs using 3-D structures of ligands and receptors provides unique insights into pharmacophore features of agonists and antagonists. The key pharmacophore elements for agonist binding, found from superposition of peptide and nonpeptide agonists inside the receptor binding pocket (Figures 3 and 4), include (1) positively charged amine ("N^+") interacting with Asp(3.32) and, for peptides, with Tyr(3.33); (2) aromatic ring of tyramine ("A") forming "stacking" interactions with Trp(6.48); (3) the central hydrophobic core ("C") interacting with TM6 residues; and (4) the second aromatic ring ("F"). The aromatic ring "F" in μ-agonists forms essential aromatic interactions with Trp318(7.35). In κ-agonists, ring "F" can be smaller, because the corresponding space in KOR near Tyr312(7.35) is smaller and more polar. In δ-agonists, ring "F" may be shifted or may extend the central hydrophobic region (to "C1"), in order to form aromatic interactions with Trp284(6.58), which serves as the functional counterpart to Trp318(7.35) of MOR. The presence of polar groups (eg, hydroxyl of tyramine, hydroxyl or carbonyl at C-6, C-14 in opiates, 2'-OH of ohmefentanyl) can additionally contribute to the binding affinity of agonists. The key pharmacophore elements for antagonists (Figures 1 and 5) include (1) positively charged ("N^+") forming weaker ionic interactions with the more distant Asp(3.32) and amine-aromatic interactions with Tyr(3.33); (2) phenolic ring ("A") forming H-bond with His(6.52); (3) the central hydrophobic core ("C") contacting residues from TM3 and TM6; and (4) additional hydrophobic elements near N^+ ("D"), which can lock Trp(6.48) in the "inactive" orientation. The presence of polar groups (hydroxyl at C-14, positively charged groups for κ-ligands) or an aromatic moiety ("C1") for δ-ligands can additionally contribute to antagonist binding affinity.

In contrast to previously developed ligand-based pharmacophore models of opioid ligands[156-159] these ligand and receptor-derived pharmacophore models not only clarify the available SAR of agonists and antagonists but suggest the role of specific ligand groups in the context of receptor structure and provide novel insights into aspects of the receptor environment that have not been previously explored.

CONCLUSIONS

The examples presented above demonstrate that accurate models of MOR, DOR, and KOR can be obtained using homology modeling based on the crystal structure of rhodopsin and distance geometry refinement with experimentally-derived constraints. Experimental information is required to verify the problematic areas, such as helix distortions and divergent extracellular loops included in the binding pocket. The incorporation of available constraints appropriate for distinct functional receptor states allows modeling of the inactive and agonist-activated receptor conformations separately. Accurate ligand docking guided by experimental ligand-receptor restraints helps explain the known SAR of opioid ligands and the differences between ligand-receptor

interactions of peptide and nonpeptide agonists, as well as between agonists and antagonists. The resulting more complete and more contextual ligand and receptor-based pharmacophore models of agonists and antagonists should provide considerable advantages for rational design of compounds directed toward specific physiological responses.

ACKNOWLEDGMENTS

The authors are grateful to Dr Andrei Lomize for helpful discussions. These studies were supported by grant DA03910 from the National Institute on Drug Abuse (HIM) and University of Michigan College of Pharmacy Upjohn Research Award (IP).

REFERENCES

1. Kieffer BL. Recent advances in molecular recognition and signal transduction of active peptides: receptors for opioid peptides. *Cell Mol Neurobiol*. 1995;15:615-635.

2. Waldhoer M, Bartlett SE, Whistler JL. Opioid receptors. *Annu Rev Biochem*. 2004;73:953-990.

3. Pasternak GW. Multiple opiate receptors: déjà vu all over again. *Neuropharmacology*. 2004;47:312-323.

4. Vaccarino AL, Kastin AJ. Endogenous opiates: 2000. *Peptides*. 2001;22:2257-2328.

5. Hruby VJ, Agnes RS. Conformation-activity relationships of opioid peptides with selective activities at opioid receptors. *Biopolymers*. 1999;51:391-410.

6. Mansour A, Hoversten MT, Taylor LP, Watson SJ, Akil H. The cloned mu, delta and kappa receptors and their endogenous ligands: evidence for two opioid peptide recognition cores. *Brain Res*. 1995;700:89-98.

7. Mosberg HI, Hurst R, Hruby VJ, et al. Conformationally constrained cyclic enkephalin analogs with pronounced delta opioid receptor agonist selectivity. *Life Sci*. 1983;32:2565-2569.

8. Pelton JT, Gulya K, Hruby VJ, Duckles S, Yamamura HI. Somatostatin analogs with affinity for opiate receptors in rat brain binding assay. *Peptides*. 1985;6:159-163.

9. Pelton JT, Kazmierski W, Gulya K, Yamamura HI, Hruby VJ. Design and synthesis of conformationally constrained somatostatin analogues with high potency and specificity for mu opioid receptors. *J Med Chem*. 1986;29:2370-2375.

10. Kawasaki AM, Knapp RJ, Walton A, et al. Syntheses, opioid binding affinities, and potencies of dynorphin A analogues substituted in positions 1, 6, 7, 8, and 10. *Int J Pept Protein Res*. 1993;42:411-419.

11. Meyer JP, Collins N, Lung FD, et al. Design, synthesis, and biological properties of highly potent cyclic dynorphin A analogues: analogues cyclized between positions 5 and 11. *J Med Chem*. 1994;37:3910-3917.

12. Arttamangkul S, Murray TF, DeLander GE, Aldrich JV. Synthesis and opioid activity of conformationally constrained dynorphin A analogues. 1. Conformational constraint in the "message" sequence. *J Med Chem*. 1995;38:2410-2417.

13. Lung FD, Collins N, Stropova D, et al. Design, synthesis, and biological activities of cyclic lactam peptide analogues of dynorphin A(1-11)-NH2. *J Med Chem*. 1996;39:1136-1141.

14. Eguchi M. Recent advances in selective opioid receptor agonists and antagonists. *Med Res Rev*. 2004;24:182-212.

15. Okada T, Ernst OP, Palczewski K, Hofmann KP. Activation of rhodopsin: new insights from structural and biochemical studies. *Trends Biochem Sci*. 2001;26:318-324.

16. Li J, Edwards PC, Burghammer M, Villa C, Schertler GF. Structure of bovine rhodopsin in a trigonal crystal form. *J Mol Biol*. 2004;343:1409-1438.

17. Flower DR. Modeling G-protein-coupled receptors for drug design. *Biochim Biophys Acta*. 1999;1422:207-234.

18. Flippen-Anderson JL, George C, Bertha CM, Rice KC. X-ray structure of potent opioid receptor ligands: etonitazene, cis-(+)-3-methylfentanyl, etorphine, diprenorphine, and buprenorphine. *Heterocycles*. 1994;39:751-766.

19. Urbanczyk-Lipkowska Z, Etter MC, Lipkowski AW, Portoghese PS. The crystal structure of a bimorphinan with highly selective kappa opioid receptor antagonist activity. *J Mol Struct*. 1987;159:287-295.

20. Griffin JF, Larson DL, Portoghese PS. Crystal structures of alpha- and beta-funaltrexamine: conformational requirement of the fumaramate moiety in the irreversible blockage of mu opioid receptors. *J Med Chem*. 1986;29:778-783.

21. Calderon SN, Rice KC, Rothman RB, et al. Probes for narcotic receptor mediated phenomena. 23. Synthesis, opioid receptor binding, and bioassay of the highly selective delta agonist (+)-4-[(alpha R)-alpha-((2S,5R)-4-Allyl-2,5-dimethyl-1-piperazinyl)-3-methoxybenzyl]-N,N-diethylbenzamide (SNC 80) and related novel nonpeptide delta opioid receptor ligands. *J Med Chem*. 1997;40:695-704.

22. Lavecchia A, Greco G, Novellino E, Vittorio F, Ronsisvalle G. Modeling of kappa-opioid receptor/agonists interactions using pharmacophore-based and docking simulations. *J Med Chem*. 2000;43:2124-2134.

23. Doi M, Ishida T, Inoue M. Conformational characteristics of opioid kappa-receptor agonist: crystal structure of (5S,7S,8S)-(-)-N-methyl-N-[7-(1-pyrrolidinyl)-1-oxaspiro[4.5]dec-8-yl]benzeneacetamide (U69,593), and conformational comparison with some kappa-agonists. *Chem Pharm Bull (Tokyo)*. 1990;38:1815-1818.

24. Subramanian G, Patrelini MG, Portoghese PS, Ferguson DM. Molecular docking reveals a novel binding site model for fentanyl at the mu-opioid receptor. *J Med Chem*. 2000;43:381-391.

25. Mosberg HI, Fowler CB. Development and validation of opioid ligand-receptor interaction models: the structural basis of mu vs delta selectivity. *J Pept Res*. 2002;60:329-335.

26. Przydzial MJ, Pogozheva ID, Andrews SM, et al. Roles of residues 3 and 4 in cyclic tetrapeptide ligand recognition by the κ-opioid receptor. *J Pept Res*. 2005;65:333-342.

27. Mosberg HI, Omnaas JR, Medzihradsky F, Smith CB. Cyclic, disulfide- and dithioether-containing opioid tetrapeptides: development of a ligand with high delta opioid receptor selectivity and affinity. *Life Sci*. 1988;43:1013-1020.

28. Mosberg HI, Lomize AL, Wang C, et al. Development of a model for the δ-opioid receptor pharmacophore. 1. Conformationally restricted Tyr^1 replacements in the cyclic δ receptor selective tetrapeptide Tyr-c[D-Cys-Phe-D-Pen]OH (JOM-13). *J Med Chem*. 1994*a*;37:4371-4383.

29. Mosberg HI, Omnaas JR, Lomize A, et al. Development of a model for the δ-opioid receptor pharmacophore. 2. Conformationally restricted Phe^3 replacements in the cyclic δ-receptor selective tetrapeptide Tyr-c[D-Cys-Phe-D-Pen]OH (JOM-13). *J Med Chem*. 1994*b*;37:4384-4391.

30. Mosberg HI, Dua RK, Pogozheva ID, Lomize AL. Development of a model for the δ-opioid receptor pharmacophore. 4. Residue 3

dehydrophenyl-alanine analogs of Tyr-c[D-Cys-Phe-D-Pen]OH (JOM-13) confirm required gauche orientation of aromatic sidechain. *Biopolymers*. 1996;39:287-296.

31. Lomize AL, Flippen-Anderson JL, George C, Mosberg HI. Conformational analysis of the δ receptor-selective, cyclic opioid peptide,Tyr-c[D-Cys-Phe-D-Pen]OH(JOM-13): comparison of X-ray crystallographic structures, molecular mechanics simulations and ^{1}H NMR data. *J Am Chem Soc*. 1994;116:429-436.

32. Ho JC. *Development of a Model for the* δ*-opioid Receptor Pharmacophore* [dissertation]. Ann Arbor, MI: University of Michigan; 1997.

33. McFadyen IJ, Ho JC, Mosberg HI, Traynor JR. Modifications of the cyclic mu receptor selective tetrapeptide Tyr-c[D-Cys-Phe-D-Pen]NH2 (Et): effects on opioid receptor binding and activation. *J Pept Res*. 2000;55:255-261.

34. Fowler CB III, Pogozheva ID III, Lomize AL III, LeVine H III, Mosberg HI. Complex of an active μ-opioid receptor with cyclic peptide agonist modeled from experimental constraints. *Biochemistry*. 2004*a*;43:15796-15810.

35. Mosberg HI. Complementarity of delta opioid ligand pharmacophore and receptor models. *Biopolymers*. 1999;51:426-439.

36. Law PY, Loh HH. Regulation of opioid receptor activities. *J Pharmacol Exp Ther*. 1999;289:607-624.

37. Chaturvedi K, Christoffers KH, Singh K, Howells RD. Structure and regulation of opioid receptors. *Biopolymers*. 2000;55:334-346.

38. Chavkin C, McLaughlin JP, Celver JP. Regulation of opioid receptor function by chronic agonist exposure: constitutive activity and desensitization. *Mol Pharmacol*. 2001;60:20-25.

39. Coward P, Wada HG, Falk MS, et al. Controlling signaling with a specifically designed Gi-coupled receptor. *Proc Natl Acad Sci USA*. 1998;95:352-357.

40. Pogozheva ID, Lomize AL, Mosberg HI. Opioid receptor 3-dimensional structures from distance geometry calculations with hydrogen bonding constraints. *Biophys J*. 1998;75:612-634.

41. Surratt CK, Johnson PS, Moriwaki A, et al. Mu opiate receptor: charged transmembrane domain amino acids are critical for agonist recognition and intrinsic activity. *J Biol Chem*. 1994;269:20548-20553.

42. Befort K, Tabbara L, Bausch S, Chavkin C, Evans C, Kieffer BL. The conserved aspartate residue in the third putative transmembrane domain of the delta-opioid receptor is not the anionic counterpart for cationic opiate binding but is a constituent of the receptor binding site. *Mol Pharmacol*. 1996*a*;49:216-223.

43. Befort K, Tabbara L, Kling D, Maigret B, Kieffer BL. Role of aromatic transmembrane residues of the delta-opioid receptor in ligand recognition. *J Biol Chem*. 1996*b*;271:10161-10168.

44. Befort K, Zilliox C, Filliol D, Yue S, Kieffer BL. Constitutive activation of the delta opioid receptor by mutations in transmembrane domains III and VII. *J Biol Chem*. 1999;274:18574-18581.

45. Bot G, Blake AD, Li S, Reisine T. Mutagenesis of the mouse delta opioid receptor converts (-)-buprenorphine from a partial agonist to an antagonist. *J Pharmacol Exp Ther*. 1998*a*;284:283-290.

46. Bot G, Blake AD, Li S, Reisine T. Mutagenesis of a single amino acid in the rat mu-opioid receptor discriminates ligand binding. *J Neurochem*. 1998*b*;70:358-365.

47. Spivak CE, Beglan CL, Seidleck BK, et al. Naloxone activation of mu-opioid receptors mutated at a histidine residue lining the opioid binding cavity. *Mol Pharmacol*. 1997;52:983-992.

48. Mansour A, Taylor LP, Fine JL, et al. Key residues defining the mu-opioid receptor binding pocket: a site-directed mutagenesis study. *J Neurochem*. 1997;68:344-353.

49. Meng F, Ueda Y, Hoversten MT, et al. Creating a functional opioid alkaloid binding site in the orphanin FQ receptor through site-directed mutagenesis. *Mol Pharmacol*. 1998;53:772-777.

50. Li JG, Chen C, Yin J, et al. ASP147 in the third transmembrane helix of the rat mu opioid receptor forms ion-pairing with morphine and naltrexone. *Life Sci*. 1999;65:175-185.

51. Fukuda K, Terasako K, Kato S, Mori K. Identification of the amino acid residues involved in selective agonist binding in the first extracellular loop of the delta- and mu-opioid receptors. *FEBS Lett*. 1995;373:177-181.

52. Minami M, Onogi T, Nakagawa T, et al. DAMGO, a mu-opioid receptor selective ligand, distinguishes between mu-and kappa-opioid receptors at a different region from that for the distinction between mu- and delta-opioid receptors. *FEBS Lett*. 1995;364:23-27.

53. Wang JB, Johnson PS, Wu JM, Wang WF, Uhl GR. Human kappa opiate receptor second extracellular loop elevates dynorphin's affinity for human mu/kappa chimeras. *J Biol Chem*. 1994;269:25966-25969.

54. Xue JC, Chen C, Zhu J, et al. Differential binding domains of peptide and non-peptide ligands in the cloned rat kappa opioid receptor. *J Biol Chem*. 1994;269:30195-30199.

55. Ferguson DM, Kramer S, Metzger TG, Law PY, Portoghese PS. Isosteric replacement of acidic with neutral residues in extracellular loop-2 of the kappa-opioid receptor does not affect dynorphin A(1-13) affinity and function. *J Med Chem*. 2000;43:1251-1252.

56. Bonner G, Meng F, Akil H. Selectivity of mu-opioid receptor determined by interfacial residues near third extracellular loop. *Eur J Pharmacol*. 2000;403:37-44.

57. Xu H, Lu YF, Partilla JS, et al. Opioid peptide receptor studies. 11. Involvement of Tyr148, Trp318 and His319 of the rat mu-opioid receptor in binding of mu-selective ligands. *Synapse*. 1999;32:23-28.

58. Ulens C, Van Boven M, Daenens P, Tytgat J. Interaction of p-fluorofentanyl on cloned human opioid receptors and exploration of the role of Trp-318 and His-319 in mu-opioid receptor selectivity. *J Pharmacol Exp Ther*. 2000;294:1024-1033.

59. Pepin MC, Yue SY, Roberts E, Wahlestedt C, Walker P. Novel "restoration of function" mutagenesis strategy to identify amino acids of the delta-opioid receptor involved in ligand binding. *J Biol Chem*. 1997;272:9260-9267.

60. Valiquette M, Vu HK, Yue SY, Wahlestedt C, Walker P. Involvement of Trp-284, Val-296, and Val-297 of the human delta-opioid receptor in binding of delta-selective ligands. *J Biol Chem*. 1996;271:18789-18796.

61. Hjorth SA, Thirstrup K, Grandy DK, Schwartz TW. Analysis of selective binding epitopes for the kappa-opioid receptor antagonist nor-binaltorphimine. *Mol Pharmacol*. 1995;47:1089-1094.

62. Cavalli A, Babey AM, Loh HH. Altered adenylyl cyclase responsiveness subsequent to point mutations of Asp 128 in the third transmembrane domain of the delta-opioid receptor. *Neuroscience*. 1999;93:1025-1031.

63. Li J, Huang P, Chen C, de Riel JK, Weinstein H, Liu-Chen LY. Constitutive activation of the mu opioid receptor by mutation of D3.49(164), but not D3.32(147): D3.49(164) is critical for stabilization of the inactive form of the receptor and for its expression. *Biochemistry*. 2001;40:12039-12050.

64. Mouledous L, Topham CM, Moisand C, Mollereau C, Meunier JC. Functional inactivation of the nociceptin receptor by alanine substitution of glutamine 286 at the C terminus of transmembrane segment VI: evidence from a site-directed mutagenesis study of the ORL1 receptor transmembrane-binding domain. *Mol Pharmacol*. 2000;57:495-502.

65. DeCaillot FM, Befort K, Filliol D, Yue S, Walker P, Kieffer BL. Opioid receptor random mutagenesis reveals a mechanism for G protein-coupled receptor activation. *Nat Struct Biol*. 2003;10:629-636.

66. Spivak CE, Beglan CL, Zollner C, Surratt CK. Beta-Funaltrexamine, a gauge for the recognition site of wildtype and mutant H297Q mu-opioid receptors. *Synapse*. 2003;49:55-60.

67. Chen C, Yin J, Riel JK, et al. Determination of the amino acid residue involved in [3H]beta-funaltrexamine covalent binding in the cloned rat mu-opioid receptor. *J Biol Chem*. 1996;271:21422-21429.

68. Jones RM, Hjorth SA, Schwartz TW, Portoghese PS. Mutational evidence for a common kappa antagonist binding pocket in the wild-type kappa and mutant mu[K303E] opioid receptors. *J Med Chem*. 1998;41:4911-4914.

69. Larson DL, Jones RM, Hjorth SA, Schwartz TW, Portoghese PS. Binding of norbinaltorphimine (norBNI) congeners to wild-type and mutant mu and kappa opioid receptors: molecular recognition loci for the pharmacophore and address components of kappa antagonists. *J Med Chem*. 2000;43:1573-1576.

70. Fowler CB III, Pogozheva ID III, LeVine H III, Mosberg HI. Refinement of a homology model of the μ-opioid receptor using distance constraints from intrinsic and engineered zinc-binding sites. *Biochemistry*. 2004*b*;43:8700-8710.

71. Metzger TG, Paterlini MG, Portoghese PS, Ferguson DM. An analysis of the conserved residues between halobacterial retinal proteins and G-protein coupled receptors: implications for GPCR modeling. *J Chem Inf Comput Sci*. 1996;36:857-861.

72. Strahs D, Weinstein H. Comparative modeling and molecular dynamics studies of the delta, kappa and mu opioid receptors. *Protein Eng*. 1997;10:1019-1038.

73. Alkorta I, Loew GH. A 3D model of the delta opioid receptor and ligand-receptor complexes. *Protein Eng*. 1996;9:573-583.

74. Subramanian G, Paterlini MG, Larson DL, Portoghese PS, Ferguson DM. Conformational analysis and automated receptor docking of selective arylacetamide-based kappa-opioid agonists. *J Med Chem*. 1998;41:4777-4789.

75. Paterlini G, Portoghese PS, Ferguson DM. Molecular simulation of dynorphin A-(1-10) binding to extracellular loop 2 of the kappa-opioid receptor: a model for receptor activation. *J Med Chem*. 1997;40:3254-3262.

76. Filizola M, Laakkonen L, Loew GH. 3D modeling, ligand binding and activation studies of the cloned mouse delta, mu, and kappa opioid receptors. *Protein Eng*. 1999*a*;12:927-942.

77. Filizola M, Carteni-Farina M, Perez JJ. Molecular modeling study of the differential ligand-receptor interaction at the mu, delta and kappa opioid receptors. *J Comput Aided Mol Des*. 1999*b*;13:397-407.

78. Pogozheva ID, Lomize AL, Mosberg HI. The transmembrane 7 alpha-bundle of rhodopsin: distance geometry calculations with hydrogen bonding constraints. *Biophys J*. 1997;72:1963-1985.

79. Lomize AL, Pogozheva ID, Mosberg HI. Structural organization of G-protein-coupled receptors. *J Comput Aided Mol Des*. 1999;13:325-353.

80. Vaidehi N, Floriano WB, Trabanino R, et al. Prediction of structure and function of G protein-coupled receptors. *Proc Natl Acad Sci USA*. 2002;99:12622-12627.

81. Shacham S, Topf M, Avisar N, et al. Modeling the 3D structure of GPCRs from sequence. *Med Res Rev*. 2001;21:472-483.

82. Shi L, Javitch JA. The binding site of aminergic G protein-coupled receptors: the transmembrane segments and second extracellular loop. *Annu Rev Pharmacol Toxicol*. 2002;42:437-467.

83. Lawson Z, Wheatley M. The third extracellular loop of G-protein-coupled receptors: more than just a linker between 2 important transmembrane helices. *Biochem Soc Trans*. 2004;32:1048-1050.

84. Baker D, Sali A. Protein structure prediction and structural genomics. *Science*. 2001;294:93-96.

85. Palczewski K, Kumasaka T, Hori T, et al. Crystal structure of rhodopsin: a G protein-coupled receptor. *Science*. 2000;289:739-745.

86. Ballesteros JA, Shi L, Javitch JA. Structural mimicry in G protein-coupled receptors: implications of the high-resolution structure of rhodopsin for structure-function analysis of rhodopsin-like receptors. *Mol Pharmacol*. 2001;60:1-19.

87. Klabunde T, Hessler G. Drug design strategies for targeting G-protein-coupled receptors. *ChemBioChem*. 2002;3:928-944.

88. Bissantz C, Bernard P, Hibert M, Rognan D. Protein-based virtual screening of chemical databases. II. Are homology models of G-protein coupled receptors suitable targets? *Proteins*. 2003;50:5-25.

89. Evers A, Klebe G. Ligand-supported homology modeling of g-protein-coupled receptor sites: models sufficient for successful virtual screening. *Angew Chem Int Ed Engl*. 2004*a*;43:248-251.

90. Horn F, Bettler E, Oliveira L, Campagne F, Cohen FE, Vriend G. GPCRDB information system for G protein-coupled receptors. *Nucleic Acids Res*. 2003;31:294-297.

91. Huang P, Li J, Chen C, Visiers I, Weinstein H, Liu-Chen LY. Functional role of a conserved motif in TM6 of the rat mu opioid receptor: constitutively active and inactive receptors result from substitutions of Thr6.34(279) with Lys and Asp. *Biochemistry*. 2001;40:13501-13509.

92. Sali A, Blundell TL. Comparative protein modeling by satisfaction of spatial restraints. *J Mol Biol*. 1993;234:779-815.

93. Fiser A, Sali A. Modeller: generation and refinement of homology-based protein structure models. *Methods Enzymol*. 2003;374:461-491.

94. Peitsch MC. ProMod and Swiss-Model: internet-based tools for automated comparative protein modelling. *Biochem Soc Trans*. 1996;24:274-279.

95. Lund O, Frimand K, Gorodkin J, et al. Protein distance constraints predicted by neural networks and probability density functions. *Protein Eng*. 1997;10:1241-1248.

96. 96. ShindyalovIN, BournePE. Improving alignments in HM protocol with intermediate sequences. In: Forth Meeting on the Critical Assessment of Techniques for Protein Structure Prediction; 2000: A-92.

97. Lambert C, Leonard N, De Bolle X, Depiereux E. ESyPred3D: prediction of proteins 3D structures. *Bioinformatics*. 2002;18:1250-1256.

98. Kim DE, Chivian D, Baker D. Protein structure prediction and analysis using the Robetta server. *Nucleic Acids Res*. 2004;32:W526-W531.

99. Pieper U, Eswar N, Braberg H, et al. MODBASE, a database of annotated comparative protein structure models, and associated resources. *Nucleic Acids Res*. 2004;32:D217-D222.

100. Eswar N, John B, Mirkovic N, et al. Tools for comparative protein structure modeling and analysis. *Nucleic Acids Res*. 2003;31:3375-3380.

101. John B, Sali A. Comparative protein structure modeling by iterative alignment, model building and model assessment. *Nucleic Acids Res*. 2003;31:3982-3992.

102. Riek RP, Rigoutsos I, Novotny J, Graham RM. Non-alphα-helical elements modulate polytopic membrane protein architecture. *J Mol Biol*. 2001;306:349-362.

103. Fiser A, Do RK, Sali A. Modeling of loops in protein structures. *Protein Sci*. 2000;9:1753-1773.

104. Chothia C, Lesk AM. Helix movements and the reconstruction of the haem pocket during the evolution of the cytochrome c family. *J Mol Biol*. 1985;182:151-158.

105. Meng EC, Bourne HR. Receptor activation: what does the rhodopsin structure tell us? *Trends Pharmacol Sci*. 2001;22:587-593.

106. Karnik SS, Gogonea C, Patil S, Saad Y, Takezako T. Activation of G-protein-coupled receptors: a common molecular mechanism. *Trends Endocrinol Metab*. 2003;14:431-437.

107. Ghanouni P, Steenhuis JJ, Farrens DL, Kobilka BK. Agonist-induced conformational changes in the G-protein-coupling domain of the beta 2 adrenergic receptor. *Proc Natl Acad Sci USA*. 2001*a*;98:5997-6002.

108. Farrens DL, Altenbach C, Yang K, Hubbell WL, Khorana HG. Requirement of rigid-body motion of transmembrane helices for light activation of rhodopsin. *Science*. 1996;274:768-770.

109. Gether U, Lin S, Ghanouni P, Ballesteros JA, Weinstein H, Kobilka BK. Agonists induce conformational changes in transmembrane domains III and VI of the beta2 adrenoceptor. *EMBO J*. 1997;16:6737-6747.

110. Dunham TD, Farrens DL. Conformational changes in rhodopsin: movement of helix F detected by site-specific chemical labeling and fluorescence spectroscopy. *J Biol Chem*. 1999;274:1683-1690.

111. Han M, Smith SO, Sakmar TP. Constitutive activation of opsin by mutation of methionine 257 on transmembrane helix 6. *Biochemistry*. 1998;37:8253-8261.

112. Cai K, Klein-Seetharaman J, Hwa J, Hubbell WL, Khorana HG. Structure and function in rhodopsin: effects of disulfide cross-links in the cytoplasmic face of rhodopsin on transducin activation and phosphorylation by rhodopsin kinase. *Biochemistry*. 1999;38:12893-12898.

113. Ghanouni P, Gryczynski Z, Steenhuis JJ, et al. Functionally different agonists induce distinct conformations in the G protein coupling domain of the beta 2 adrenergic receptor. *J Biol Chem*. 2001*b*;276:24433-24436.

114. Janz JM, Farrens DL. Rhodopsin activation exposes a key hydrophobic binding site for the transducin alpha-subunit C terminus. *J Biol Chem*. 2004;279:29767-29773.

115. Hubbell WL, Altenbach C, Hubbell CM, Khorana HG. Rhodopsin structure, dynamics, and activation: a perspective from crystallography, site-directed spin labeling, sulfhydryl reactivity, and disulfide cross-linking. *Adv Protein Chem*. 2003;63:243-290.

116. Lin SW, Sakmar TP. Specific tryptophan UV-absorbance changes are probes of the transition of rhodopsin to its active state. *Biochemistry*. 1996;35:11149-11159.

117. Altenbach C, Cai K, Khorana HG, Hubbell WL. Structural features and light-dependent changes in the sequence 306-322 extending from helix VII to the palmitoylation sites in rhodopsin: a site-directed spin-labeling study. *Biochemistry*. 1999*a*;38:7931-7937.

118. Altenbach C, Klein-Seetharaman J, Hwa J, Khorana HG, Hubbell WL. Structural features and light-dependent changes in the sequence 59-75 connecting helices I and II in rhodopsin: a site-directed spin-labeling study. *Biochemistry*. 1999*b*;38:7945-7949.

119. Altenbach C, Cai K, Klein-Seetharaman J, Khorana HG, Hubbell WL. Structure and function in rhodopsin: mapping light-dependent changes in distance between residue 65 in helix TM1 and residues in the sequence 306-319 at the cytoplasmic end of helix TM7 and in helix H8. *Biochemistry*. 2001*a*;40:15483-15492.

120. Altenbach C, Klein-Seetharaman J, Cai K, Khorana HG, Hubbell WL. Structure and function in rhodopsin: mapping light-dependent changes in distance between residue 316 in helix 8 and residues in the sequence 60-75, covering the cytoplasmic end of helices TM1 and TM2 and their connection loop CL1. *Biochemistry*. 2001*b*;40:15493-15500.

121. Gether U, Kobilka BK. G protein-coupled receptors. II. Mechanism of agonist activation. *J Biol Chem*. 1998;273:17979-17982.

122. Devanathan S, Yao Z, Salamon Z, Kobilka B, Tollin G. Plasmon-waveguide resonance studies of ligand binding to the human beta 2-adrenergic receptor. *Biochemistry*. 2004;43:3280-3288.

123. Salamon Z, Cowell S, Varga E, Yamamura HI, Hruby VJ, Tollin G. Plasmon resonance studies of agonist/antagonist binding to the human delta-opioid receptor: new structural insights into receptor-ligand interactions. *Biophys J*. 2000;79:2463-2474.

124. Salamon Z, Hruby VJ, Tollin G, Cowell S. Binding of agonists, antagonists and inverse agonists to the human delta-opioid receptor produces distinctly different conformational states distinguishable by plasmon-waveguide resonance spectroscopy. *J Pept Res*. 2002;60:322-328.

125. Alves ID, Ciano KA, Boguslavski V, et al. Selectivity, cooperativity, and reciprocity in the interactions between the delta-opioid receptor, its ligands, and G-proteins. *J Biol Chem*. 2004*a*;279:44673-44682.

126. Alves ID, Cowell SM, Salamon Z, Devanathan S, Tollin G, Hruby VJ. Different structural states of the proteolipid membrane are produced by ligand binding to the human delta-opioid receptor as shown by plasmon-waveguide resonance spectroscopy. *Mol Pharmacol*. 2004*b*;65:1248-1257.

127. Tramontano A, Morea V. Exploiting evolutionary relationships for predicting protein structures. *Biotechnol Bioeng*. 2003;84:756-762.

128. Bates PA, Kelley LA, MacCallum RM, Sternberg MJ. Enhancement of protein modeling by human intervention in applying the automatic programs 3D-JIGSAW and 3D-PSSM. *Proteins*. 2001;39-46.

129. Li X, Jacobson MP, Friesner RA. High-resolution prediction of protein helix positions and orientations. *Proteins*. 2004;55:368-382.

130. Evers A, Gohlke H, Klebe G. Ligand-supported homology modelling of protein binding-sites using knowledge-based potentials. *J Mol Biol*. 2003;334:327-345.

131. Ward SD, Hamdan FF, Bloodworth LM, Wess J. Conformational changes that occur during M3 muscarinic acetylcholine receptor activation probed by the use of an in situ disulfide cross-linking strategy. *J Biol Chem*. 2002;277:2247-2257.

132. Swaminath G, Lee TW, Kobilka B. Identification of an allosteric binding site for Zn^{2+} on the beta2 adrenergic receptor. *J Biol Chem*. 2003;278:352-356.

133. Elling CE, Thirstrup K, Holst B, Schwartz TW. Conversion of agonist site to metal-ion chelator site in the beta(2)-adrenergic receptor. *Proc Natl Acad Sci USA*. 1999;96:12322-12327.

134. Holst B, Elling CE, Schwartz TW. Partial agonism through a zinc-ion switch constructed between transmembrane domains III and VII in the tachykinin NK(1) receptor. *Mol Pharmacol*. 2000;58:263-270.

135. Lagerstrom MC, Klovins J, Fredriksson R, et al. High affinity agonistic metal ion binding sites within the melanocortin 4 receptor illustrate conformational change of transmembrane region 3. *J Biol Chem*. 2003;278:51521-51526.

136. Ewing TJ, Makino S, Skillman AG, Kuntz ID. DOCK 4.0: search strategies for automated molecular docking of flexible molecule databases. *J Comput Aided Mol Des*. 2001;15:411-428.

137. Jones G, Willett P, Glen RC, Leach AR, Taylor R. Development and validation of a genetic algorithm for flexible docking. *J Mol Biol*. 1997;267:727-748.

138. Rarey M, Wefing S, Lengauer T. Placement of medium-sized molecular fragments into active sites of proteins. *J Comput Aided Mol Des*. 1996;10:41-54.

139. Taylor RD, Jewsbury PJ, Essex JW. FDS: flexible ligand and receptor docking with a continuum solvent model and soft-core energy function. *J Comput Chem*. 2003;24:1637-1656.

140. Halgren TA, Murphy RB, Friesner RA, et al. Glide: a new approach for rapid, accurate docking and scoring. 2. Enrichment factors in database screening. *J Med Chem*. 2004;47:1750-1759.

141. Venkatachalam CM, Jiang X, Oldfield T, Waldman M. LigandFit: a novel method for the shape-directed rapid docking of ligands to protein active sites. *J Mol Graph Model*. 2003;21:289-307.

142. Cavasotto CN, Abagyan RA. Protein flexibility in ligand docking and virtual screening to protein kinases. *J Mol Biol*. 2004;337:209-225.

143. Perola E, Walters WP, Charifson PS. A detailed comparison of current docking and scoring methods on systems of pharmaceutical relevance. *Proteins*. 2004;56:235-249.

144. Halperin I, Ma B, Wolfson H, Nussinov R. Principles of docking: an overview of search algorithms and a guide to scoring functions. *Proteins*. 2002;47:409-443.

145. Kontoyianni M, McClellan LM, Sokol GS. Evaluation of docking performance: comparative data on docking algorithms. *J Med Chem*. 2004;47:558-565.

146. Carlson HA, McCammon JA. Accommodating protein flexibility in computational drug design. *Mol Pharmacol*. 2000;57:213-218.

147. Evers A, Klebe G. Successful virtual screening for a submicromolar antagonist of the neurokinin-1 receptor based on a ligand-supported homology model. *J Med Chem*. 2004*b*;47:5381-5392.

148. Heyl DL, Mosberg HI. Modification of the Phe3 aromatic moiety in delta receptor-selective dermorphin/deltorphin-related tetrapeptides: effects on opioid receptor binding. *Int J Pept Protein Res*. 1992;39:450-457.

149. Sebastian A, Bidlack JM, Jiang Q, et al. 14 beta-[(p-nitrocinnamoyl)amino]morphinones, 14 beta-[(p-nitrocinnamoyl)amino]-7,8-dihydromorphinones, and their codeinone analogues: synthesis and receptor activity. *J Med Chem*. 1993;36:3154-3160.

150. Sagara T, Egashira H, Okamura M, Fujii I, Shimohigashi Y, Kanematsu K. Ligand recognition in mu opioid receptor: experimentally based modeling of mu opioid receptor binding sites and their testing by ligand docking. *Bioorg Med Chem*. 1996;4:2151-2166.

151. Chabre M, Breton J. Orientation of aromatic residues in rhodopsin: rotation of one tryptophan upon the meta I to meta II transition after illumination. *Photochem Photobiol*. 1979;30:295-299.

152. Baneres JL, Martin A, Hullot P, Girard JP, Rossi JC, Parello J. Structure-based analysis of GPCR function: conformational adaptation of both agonist and receptor upon leukotriene B4 binding to recombinant BLT1. *J Mol Biol*. 2003;329:801-814.

153. Ruprecht JJ, Mielke T, Vogel R, Villa C, Schertler GF. Electron crystallography reveals the structure of metarhodopsin I. *EMBO J*. 2004;23:3609-3620.

154. Sammes PG, Taylor JB. Opioid receptors. In: Hansch C, ed. *Comprehensive Medicinal Chemistry.* Oxford, UK: Pergamon Press; 1990:805-844.

155. Schiller PW, Weltrowska G, Nguyen TM-D, Lemieux C, Chung NN, Lu Y. Conversion of μ-, δ- and κ-receptor selective opioid peptide agonists into μ-, δ-, and κ-receptor selective antagonists. *Life Sci*. 2003;73:691-698.

156. Huang P, Kim S, Loew G. Development of a common 3D pharmacophore for delta-opioid recognition from peptides and non-peptides using a novel computer program. *J Comput Aided Mol Des*. 1997;11:21-28.

157. Filizola M, Villar HO, Loew GH. Molecular determinants of non-specific recognition of delta, mu, and kappa opioid receptors. *Bioorg Med Chem*. 2001*a*;9:69-76.

158. Filizola M, Villar HO, Loew GH. Differentiation of delta, mu, and kappa opioid receptor agonists based on pharmacophore development and computed physicochemical properties. *J Comput Aided Mol Des*. 2001*b*;15:297-307.

159. Bernard D Jr, Coop A Jr, MacKerell AD Jr. 2D conformationally sampled pharmacophore: a ligand-based pharmacophore to differentiate delta opioid agonists from antagonists. *J Am Chem Soc*. 2003;125:3101-3107.